Ott, F., Kramkowski, M., Wulf, S., Plessen, B., Serb, J., Tjallingii, R., Schwab, M. J., Slowinski, M., Brykala, D., Tyszkowski, S., Putyrskaya, V., Appelt, O., Błaszkiewicz, M., Brauer, A. (2018): Site-specific sediment responses to climate change during the last 140 years in three varved lakes in Northern Poland. - *Holocene*, *28*, 3.

DOI: http://doi.org/10.1177/0959683617729448

Research paper

Site-specific sediment responses to climate change during the last 140 years in three varved lakes in Northern Poland

The Holocene
2018, Vol. 28(3) 464–477

Reprints and permissions:
sagepub.co.uk/journalsPermissions.nav
DOI: 10.1177/0959683617729448
journals.sagepub.com/home/hol
SAGE

Florian Ott,[1,2] Mateusz Kramkowski,[1,3] Sabine Wulf,[1,4] Birgit Plessen,[1] Johanna Serb,[1] Rik Tjallingii,[1] Markus Schwab,[1] Michał Słowiński,[1,3] Dariusz Brykała,[1,3] Sebastian Tyszkowski,[3] Victoria Putyrskaya,[5] Oona Appelt,[6] Miroslaw Błaszkiewicz[3] and Achim Brauer[1]

Abstract
Accurate dating and unambiguous chronological correlation using cryptotephras provide a powerful tool to compare the varved sediment records of the lakes Głęboczek (JG), Czechowskie (JC) and Jelonek (JEL) (north-central Poland). For the last 140 years, micro-facies analyses and µ-XRF element scanning at seasonal resolution, as well as bulk elemental analyses (organic matter, carbonate) at sub-decadal to decadal resolution, were conducted for all three lakes records. All lakes are located in a region with low population density, and therefore, anthropogenic influences are negligible or only minor. The varve chronologies have been established independently for each record and were synchronized with the Askja AD 1875 cryptotephra. Comparison with monthly temperature data since 1870 and daily temperature data since 1951 revealed different responses of lake deposition to recent climate change. Varves are well preserved over the entire 140 years only at JG, while in the JC record two faintly varved intervals are intercalated and in the JEL record two non-varved intervals occur at the base and top of the profiles. These differences likely are due to variations in lake characteristics and their influence on lake-internal responses. JG is the smallest and best wind-sheltered lake, which favours varve preservation. JC's attenuated sediment responses can likely be linked to lake productivity changes with respect to climate warming. JEL is lacking a direct sedimentological response to the observed temperature increase, which can be linked to lake size and water depth superimposing regional climate changes. Climate changes at the demise of the 'Little Ice Age' around 1900 and the recent warming since the 1980s are expressed in sediment proxies in the lakes with different response times and amplitudes. This detailed comparison study on three nearby lakes demonstrates the influence of local parameters such as lake and catchment size and water depth superimposed on more regional climate-driven changes.

Keywords
Askja AD 1875 cryptotephra, climate change, ICLEA, north-central Poland, sediment response, varved lake sediments

Received 17 March 2017; revised manuscript accepted 14 July 2017

Introduction

Annually laminated (varved) lake sediments document past climate and environmental changes at high resolution beyond instrumental time series on independent and robust chronologies (Brauer et al., 1999a, 2008; Czymzik et al., 2013; Martin-Puertas et al., 2012; Zolitschka et al., 2015). They provide information especially on the timing, duration and rates of change within the human habitat (Brauer, 2004; Ojala et al., 2012; Tylmann et al., 2013; Zolitschka et al., 2015). However, lake sediment proxies respond not solely to regional variability but also to local effects controlled by site-specific factors (Bonk et al., 2016; Dräger et al., 2017; Kämpf et al., 2014; Neugebauer et al., 2015; Pędziszewska et al., 2015). Therefore, it is an essential prerequisite for interpreting past climate changes from lake sediments to disentangle regional and local proxy signals. One approach to detect the role of local effects is the comparison of lake sediment records in close vicinity to each other (Olsen et al., 2012; Roberts et al., 2016). The few available studies following this approach, however, focused on millennial-scale variability but not on decadal-scale changes. A major challenge for comparing lake records at great detail is a precise synchronization independent from proxy data, for example, through the use of volcanic ash (tephra) layers (Lowe, 2011). Recent advances in the detection of macroscopically non-visible tephra (cryptotephra) have been proven suitable for lake record synchronization (Davies, 2015;

[1]Section 5.2: Climate Dynamics and Landscape Evolution, GFZ German Research Centre for Geosciences, Germany
[2]Department of Archaeology, Max Planck Institute for the Science of Human History, Germany
[3]Department of Environmental Resources and Geohazards, Institute of Geography and Spatial Organization of the Polish Academy of Sciences, Poland
[4]Institute of Earth Sciences, Heidelberg University, Germany
[5]University of Applied Sciences Ravensburg-Weingarten, Germany
[6]Section 4.3: Chemistry and Physics of Earth Materials, GFZ German Research Centre for Geosciences, Germany

Corresponding author:
Florian Ott, Department of Archaeology, Max Planck Institute for the Science of Human History, Kahlaische Str. 10, 07745 Jena, Germany.
Email: ott@shh.mpg.de

Lane et al., 2013; Wulf et al., 2013). So far, tephra-based synchronization of lake sediment records mainly has been applied to decipher regional differences of climate change (Lane et al., 2013; Wulf et al., 2016).

The southern Baltic lowlands spanning from north-eastern Germany and Poland to the Baltic States are of particular interest for climate research because this region covers the transitional zone between Atlantic Westerlies and continental Siberian air masses. The interplay of these large-scale atmospheric circulation patterns explains up to 77% of the temperature variations over the Polish area (Degirmendžić et al., 2004; Filipiak and Mietus, 2009; Latalowa et al., 2013; Luterbacher et al., 2010; Wibig, 1999; Yu and Harrison, 1995) making Polish lake sediment records a key target for climate reconstructions (Goslar, 1995; Lauterbach et al., 2011; Ott et al., 2016; Pędziszewska et al., 2015). Some recent studies of varved lake sediments have proven site-specific factors, including increased erosion by land-use changes or strong interrelations between varve preservation and lake circulation influencing lake sedimentation (Bonk et al., 2016; Dräger et al., 2017; Wacnik et al., 2016); however, no high-resolution comparative studies of lake sediments for this region are available so far.

Here, we present the first high-resolution comparison of three neighbouring varved lake records in Northern Poland, synchronized by the Askja AD 1875 cryptotephra, covering the transition from the late 'Little Ice Age' (LIA) to the most recent warming. These lakes differ in their morphometric and bathymetric characteristics, but all are located in similar glacial till and outwash plain deposits of the last glaciation. Two of these lakes, lakes Głęboczek (JG) and Czechowskie (JC), even are located within the same catchment, while Lake Jelonek (JEL) is located only 15 km further to the South. The aim of this approach is to decipher between local (site-specific) and regional (climate) signals in sedimentological and geochemical proxy data. Ultimately, we aim at a better understanding of sediment responses to regional-scale climate and environmental changes.

Study sites

JG (53°52′N; 18°12′E; 118 m a.s.l.), JC (53°52′N; 18°14′E; 108 m a.s.l.) and JEL (53°45′N; 18°23′E; 90 m a.s.l.) are located within the Pomeranian Lakeland close to the Pomeranian ice margin dated between 17 and 16 cal. ka BP (Marks, 2012; Figure 1). Their catchments are composed of glacial till and outwash plain deposits (Błaszkiewicz, 2005; Błaszkiewicz et al., 2015; Kordowski et al., 2014; Słowiński et al., 2015). All three lake basins formed after the melting of dead ice blocks either in subglacial channels (JC and JEL) or in a kettle hole (JG). Present-day climatic conditions in north-central Poland are characterized by a warm summer continental climate. Monthly temperatures for Chojnice, the closest weather station at ca. 50 km distance from JC, range from −2.5°C in January to 17°C in July. Total annual precipitation reaches 590 mm with distinct summer maxima in July (82 mm) and August (70 mm).

JG has a maximum water depth of 18 m and, with a surface area of 7 ha, is the smallest of the three lakes (Table 1). The shoreline is covered predominantly by pine forest and some subordinated grassland in the northern part. The lake has a small inflow in the NW and an outflow to the SE. The outflow drains into the Trzechowskie palaeolake (TRZ) basin (Figure 1) from where it discharges into JC at its NW edge (Figure 1). Together with the TRZ palaeolake, JG and JC form a cascade of lakes within the same catchment and an elevation difference of 10 m (Figure 1).

JC is the deepest (32 m) and the largest (73 ha) of the study lakes (Table 1). The lake is divided in a shallow western (11 m) and a deep eastern basin (32 m), separated by a sill at 8 m water depth. The shoreline is covered by pine trees in the S and E, small settlements in the N and W and grassland and arable land in the SW, W and N of the lake (Figure 1). The lake has two small inflows entering the shallow basin in NW and N and one small outflow in the E. The sediment core has been retrieved from a small depression in the deepest basin.

JEL is located 15 km SE away from JC and surrounded by a dense pine forest (Błaszkiewicz et al., 2015; Filbrandt-Czaja, 2009). The lake covers 19 ha and has a maximum water depth of 13 m (Table 1). The lake has one outflow in the SE discharging into the Wda river (Figure 1).

Methods

Sediment coring

Surface sediment cores were retrieved from the three lakes at their deepest points using a Ghilardi gravity corer (∅: 60 mm) at JG and JC and an UWITEC gravity corer (∅: 90 mm) at JC and JEL (Table 2). The sediment cores were labelled according to the study site, year of coring and running number of obtained sediment cores. Each core was cut lengthwise into two halves (work and archive halves), documented, photographed and stored at 4°C. Core analyses included in this study are from cores JG13-K1, JC10-K2, JC10-K7, JC11-K5, JC12-K2 JEL13-K4 and JEL13-K7. JC10-K2 has been used for ^{137}Cs activity concentration measurements, JC10-K7 for varve counting and micro-facies analyses, JC11-K5 for bulk geochemistry and JC12-K2 for cryptotephra search and μ-XRF element scanning. JEL13-K4 has been used for cryptotephra identification and JEL13-K7 for varve counting and micro-facies analyses, bulk geochemistry and μ-XRF element scanning. In case of more than one core analysed from a lake (JC and JEL), a robust correlation based on distinct microscopic and macroscopic marker layers has been established.

Micro-facies analyses

Sediment slabs were cut from the working halve of the core with an overlap of 2 cm for preparing petrographic thin sections (10 cm × 2 cm) following the procedures described by Brauer and Casanova (2001). Micro-facies analyses were carried out using a petrographic microscope (Zeiss Axiophot) with varying magnifications (25×–200×) and included varve counting, total varve and varve sublayer thickness measurements, as well as sublayer compositions. Photographs of sublayers or specific sublayer components were acquired with an Olympus DP 72 microscope camera system.

Chronology

Independent dating has been established by varve counting and tephrochronology for all three lakes and ^{137}Cs activity concentration measurements for JC in order to prove annual layer counting. All ages are given in years AD.

Annual layer counting is based on precise varve and sublayer boundary definition even for intervals of low sedimentation rates. Each varve chronology is based on two independent varve counts by different investigators. Chronological uncertainties have been estimated from the deviation of the two counts (Brauer et al., 2014). Intervals with poor (JC) or even absent (JEL) varve preservation have been interpolated based on the mean sedimentation rate of 20 adjacent varves. JG and JC revealed continuous varve chronologies up to present time, and the top of the profile corresponds to the year of sediment coring (JG: 2013; JC: 2010). The JEL varve chronology is floating because of the lack of varves in the uppermost part. The floating chronology has been anchored to the Askja AD 1875 tephra and sedimentation rate of the uppermost non-varved interval has been extrapolated.

Following an earlier identification of the Askja AD 1875 tephra in the JC sediment record (Wulf et al., 2016), we applied

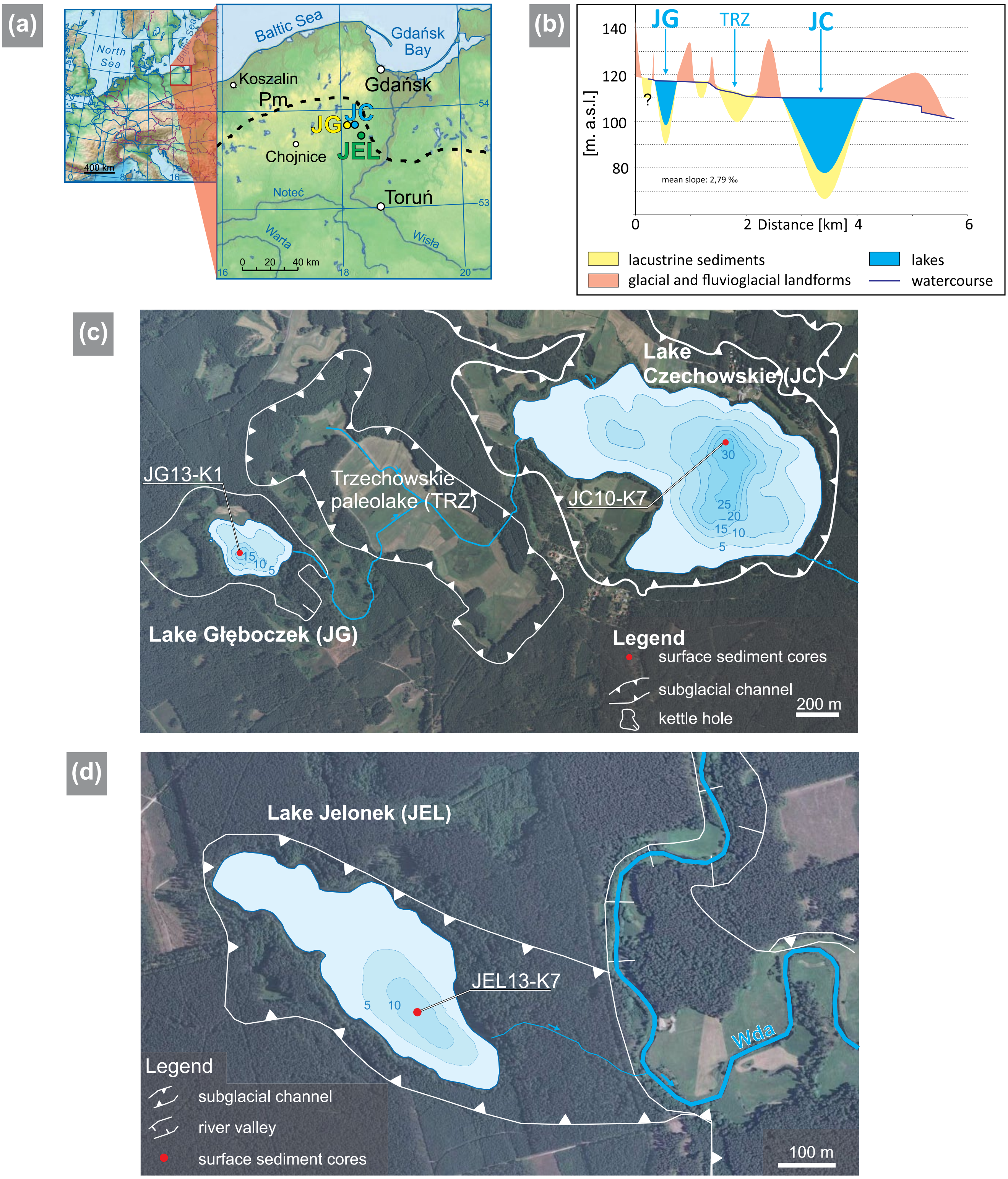

Figure 1. Overview about study sites. (a) Map of Europe and north-central Poland. The investigated lakes are marked by JG (Lake Głęboczek), JC (Lake Czechowskie) and JEL (Lake Jelonek). (b) Cross section through the lake-palaeolake cascade system with JG, palaeolake Trzechowskie (TRZ; Słowiński et al., 2017; Wulf et al., 2013) and JC. Total height difference between JG and JC is 10 m. (c and d) Aerial photographs of the study sites with simplified morphology (modified after Błaszkiewicz, 2005; Błaszkiewicz et al., 2015) and lake bathymetry. Coring locations are marked by a red dot.

the same methodological approach to search for tephra in the JG and JEL records, including (1) sampling (1 cm^3/cm) of sediment intervals selected according to preliminary varve counts, (2) separation of volcanic glass shards and (3) geochemical identification. Continuous samples were taken in 2–5 cm increments from 20 to 50 cm (JG13-K1), 15 to 74 cm (JC12-K2) and 40 to 67 cm (JEL13-K4). After initial microscopic detection of glass shards, all cores were re-sampled in 1 cm increments from 19 to 26 cm (JG13-K1), 35 to 45 cm (JC12-K2) and 38 to 55 cm (JEL13-K4). Details of chemical and physical separation of glass shards, microscopic inspection and geochemical identification are described in detail in Wulf et al. (2016). Compositional data of volcanic glass shards were re-calculated on a volatile-free basis and are summarized in Table 3 and plotted against EPMA data of potential tephra correlatives in a Harker diagram (Figure 4).

Table 1. Selected lake and catchment parameters of Lake Głęboczek (JG), Lake Czechowskie (JC) and Lake Jelonek (JEL).

	JG	JC	JEL
Location	Pomeranian Lakeland, Northern Poland		
Coordinates	53°52′N/18°12′E	53°52′N/18°14′E	53°45′N/18°23′E
Surface elevation (m a.s.l.)	118	108	91
Surface area (ha)	7	73	19.9
Catchment area (km^2)	0.65	19.7	1.11
Volume (m^3)	3.7×10^5	5.8×10^6	8.1×10^5
Maximum water depth (m)	18	32	13
Mean water depth (m)	5.33	8.08	4.1
Maximum length (m)	260	1500	880
Maximum width (m)	390	750	320

Table 2. Overview of sediment cores used for different analyses.

		Lake Głęboczek	Lake Czechowskie	Lake Jelonek
Composite profile		JG13-K1	JC10-K7	JEL13-K7
Chronology	Varve chronology	JG13-K1	JC10-K7	JEL13-K7
	Tephrochronology	JG13-K1	JC12-K2	JEL13-K4
	^{137}Cs	–	JC10-K2	–
Geochemistry	Bulk geochemistry	JG13-K1	JC11-K5	JEL13-K7
	µ-XRF	JG13-K1	JC12-K2	JEL13-K7

^{137}Cs activity concentration measurements have been carried out on continuous 2-cm sample increments of the uppermost 60 cm of core JC10-K2 at the Institute of Applied Science in Ravensburg-Weingarten with a coaxial High-Purity Germanium (HPGe) Detector of Canberra-Eurysis. Measuring time varied between 24 and 72 h per sample, depending on the activity concentration.

Geochemistry

Samples for bulk geochemical analyses (total organic carbon (TOC), total carbon (TC) and total nitrogen (TN)) were continuously taken in 1 cm intervals for JC. Because of the different sedimentation rates in the other two sediment records, JG and JEL have been sampled in 0.2–1.5 cm and 0.5–2.5 cm intervals, respectively, in order to provide a similar sub-decadal temporal resolution for the three records. All samples were freeze-dried, homogenized and analysed for carbon (TC and TOC) and nitrogen (TN) contents using elemental analyser (JC: EA3000 Eurovector; JG, JEL: NC2500 Carlo Erba). TC and TN contents were determined using 3–5 mg sample material aliquots loaded in Sn-capsules, wrapped and measured. For TOC content determination, about 2–3 mg sample aliquots were loaded in Ag-capsules, in situ decalcified (treated with 20% HCl), dried at 75°C and finally wrapped and measured. The calibration was performed using certified elemental standards and proofed with soil reference samples (HEKAtech Boden 2 and Boden 3). The reproducibility of replicate analyses is 0.2%. The $CaCO_3$ content was calculated using the following equation: total inorganic carbon content (TIC) × 8.33 (TIC = TC − TOC). The data are further normalized to *z*-scores to account for scaling effects resulting from different concentration ranges.

Semi-quantitative geochemical composition has been measured using the ITRAX µ-XRF spectrometer (Croudace et al., 2006) equipped with a chromium tube. Measurements were performed on a fresh and smooth surface of the archive halves using a step size of 200 µm, an exposure time of 10 s, a voltage of 30 kV and a current of 30 mA. Element intensities (counts per second) are displayed as log-ratios or centre-log-ratios (clr), to minimize the effects of sample geometry and matrix variations (Tjallingii et al., 2007; Weltje and Tjallingii, 2008; Weltje et al., 2015). µ-XRF results are re-calculated for annual resolution and are displayed together with their 30-year running mean.

Meteorological data

Air temperature data from the meteorological stations in Chojnice (ca. 50 km south-west of the study sites) and Koszalin (140 km north-west of the study sites) were used (Figure 2). The data from Chojnice cover the period 1951–2010 with daily resolution and are provided by the Institute of Meteorology and Water Management (IMGW). The monthly resolved Koszalin data set covers the period from 1848 to 2000 with missing data between 1930 and 1950 provided by the Global Historical Climatology Network (GHCN; Peterson and Vose, 1997; Peterson et al., 1998). Mean seasonal air temperatures (DJF, MAM, JJA and SON) have been calculated from the Koszalin data. Significant changes in mean air temperature have been detected by changes in mean and variance of the Koszalin and Chojnice data using the binary segmentation and PELT approach implemented in the R-package 'changepoint' (Killick and Eckley, 2014). To assess the number of frost days per year, all days with a mean air temperature below 0°C have been summed up for their corresponding years based on the Chojnice data (Figure 2).

Results

Sediment micro-facies

This study focused on the last 140 years, and the lower boundary of the studied sediment profiles is defined by the Askja AD 1875 tephra identified in all three sediment records. The most obvious difference appears in the sedimentation rates, which is for the study interval 24 cm in JG, but about the double in JC (48 cm) and JEL (50 cm; Figure 3).

Sediments in the JG profile are composed of finely laminated lacustrine sediments which can be divided into two lithologies (Figure 3). From 22 to 8 cm and from 2 to 0 cm, the sediment is characterized by yellowish couplets of sublayers of calcite crystals mixed with frustules of planktonic diatoms (*Stephanodiscus* spp.) and sublayers of planktonic and epiphytic diatoms and

Table 3. Individual, non-normalized major element glass data of the cryptotephras JG13-K1-23–24 cm, JC12-K2-35–36 cm and JEL13-K4-51–53 cm.

Sample	SiO_2	TiO_2	Al_2O_3	FeO	MnO	MgO	CaO	Na_2O	K_2O	P_2O_5	Total	Cl
Lake Głęboczek												
JG13-K1-23–24 cm	73.2	0.81	12.9	3.69	0.1	0.75	2.46	3.45	2.4	0.14	99.93	0.04
JG13-K1-23–24 cm	73.92	0.75	12.64	3.43	0.14	0.63	2.12	3.46	2.58	0.11	99.83	0.05
JG13-K1-23–24 cm	73.24	0.84	13.01	4.03	0.13	0.84	2.63	3.36	2.26	0.15	100.49	0.03
JG13-K1-23–24 cm	73.7	0.81	12.56	3.79	0.13	0.74	2.43	3.38	2.29	0.16	99.99	0.04
JG13-K1-23–24 cm	71.05	0.93	12.96	4.65	0.08	0.96	2.96	3.6	2.17	0.25	99.62	0.03
JG13-K1-23–24 cm	73.32	0.87	12.86	3.56	0.06	0.7	2.21	3.29	2.45	0.14	99.47	0.04
JG13-K1-23–24 cm	74.65	0.8	12.7	3.17	0.06	0.5	1.99	3.43	2.51	0.13	99.94	0.04
JG13-K1-23–24 cm	73.92	0.85	12.37	3.64	0.08	0.67	2.35	3.28	2.47	0.18	99.82	0.04
JG13-K1-23–24 cm	72.72	0.76	12.69	3.65	0.11	0.71	2.35	3.27	2.4	0.14	98.8	0.03
JG13-K1-23–24 cm	72.16	0.89	12.57	3.72	0.18	0.77	2.46	3.6	2.47	0.15	98.98	0.03
JG13-K1-23–24 cm	73.65	0.84	12.75	3.54	0.11	0.69	2.25	3.38	2.43	0.11	99.75	0.04
JG13-K1-23–24 cm	75.33	0.73	12.36	2.91	0.13	0.46	1.82	3.46	2.58	0.12	99.91	0.05
JG13-K1-23–24 cm	72.15	0.88	12.99	4.35	0.12	0.89	2.56	3.55	2.4	0.18	100.07	0.06
Lipari glass standard												
20-µm beam	73.64	0.06	13.22	1.6	0.09	0.04	0.73	3.88	5.11	0	98.37	0.35
15-µm beam	73.68	0.06	13.13	1.66	0.02	0.01	0.71	3.82	5.37	0	98.73	0.35
10-µm beam	74.87	0.08	13.16	1.53	0.07	0.05	0.72	3.9	5.11	0	99.8	0.36
Lake Czechowskie												
JC12-K2-35–36 cm	74.44	0.78	12.43	3.39	0.1	0.74	2.38	3.87	2.22	0.12	100.47	0.04
JC12-K2-35–36 cm	75.08	0.77	12.27	3.33	0.1	0.71	2.36	3.67	2.34	0.14	100.77	0.05
Lipari glass standard												
20-µm beam	75.78	0.03	12.8	1.63	0.05	0.04	0.71	3.9	5.16	0.02	100.11	0.33
15-µm beam	75.96	0.11	12.87	1.52	0.05	0.04	0.76	3.79	5.17	0.01	100.28	0.38
10-µm beam	76.06	0.07	12.95	1.45	0.06	0.06	0.72	3.73	5.07	0	100.16	0.35
Lake Jelonek												
JEL13-K4-51–53 cm	75.37	0.84	12.26	3.72	0.01	0.72	2.42	2.53	2.23	0.17	100.26	0.04
Lipari glass standard												
20-µm beam	74.64	0.1	12.55	1.43	0.05	0.05	0.75	3.89	4.85	0	98.32	0.34
15-µm beam	75.06	0.06	12.75	1.46	0.08	0.03	0.7	4	5.09	0	99.24	0.34
10-µm beam	75.07	0.11	12.75	1.45	0.06	0.02	0.74	4.02	4.87	0	99.1	0.36

organic debris interpreted as calcite varves (Brauer et al., 2008; Kelts and Hsü, 1978). Varve thickness in these units ranges between 0.5–2.8 mm/a (0–2 cm) and 0.6–6.2 mm/a (8–22 cm). From 22 cm downcore and from 8 to 2 cm, the sediment is characterized by finely laminated dark grey couplets of planktonic diatom frustules (*Stephanodiscus* spp.) mixed with chrysophyte cysts and a sublayer composed of organic debris, planktonic and epiphytic diatoms, resembling organic diatom varves (Brauer et al., 1999b). Varve thickness ranges from 0.5 to 7 mm/a (2–8 cm depth) and from 0.8 to 2.6 mm/a (22–30 cm).

The study interval in the JC record is composed of finely laminated yellowish calcite varves commonly consisting of four to five sublayers. (1) The basal sublayer is a very thin layer of chrysophyte cysts that appears in 19% of the varves. In contrast, the following four sublayers regularly occur in all varves. (2) The second sublayer consists of idiomorphic calcite and frustules of planktonic diatoms (*Stephanodiscus* spp.). (3) The third sublayer is formed by mixed (*Stephanodiscus* and *Fragiliaria* spp.) or monospecific (*Fragiliaria* spp.) diatom layers commonly mixed with patches of endogenic calcite. (4) The following sublayer is composed of epiphytic diatoms (*Navicula* spp.) and endogenic calcite patches. (5) The final sublayer of the seasonal succession is a thin mixed layer of organic debris, amorphous organic matter and scattered iron-sulphides (pyrite). In sublayer (2), we further distinguish two different calcite sublayer types. In total, 31 of the calcite sublayers exhibit a separation in a coarser grained (15–30 µm) basal and a finer grained (2–15 µm) upper layer, while the remaining 46 calcite sublayers appear as homogeneous fine-grained (2–15 µm) layer. Within the faint varved intervals, no calcite layer pattern has been distinguished. The faint varved intervals have a similar composition as the calcite varves but contain more abundant epiphytic diatoms and endogenic calcite patches indicating enhanced sediment re-deposition of littoral material. The main difference compared with the calcite varves formed in JG are (1) the formation of two calcite sublayers with different grain sizes, (2) the formation of monospecific diatom layers and (3) the deposition of a mixed sublayer marking the end of the seasonal cycle. This mixed sublayer, related to re-suspension of sediments, only occurs in JC. Between 26 and 18 cm and from 11 to 9 cm, varves are poorly preserved. Varve thickness ranges from 1.2 to 11.2 mm/a (Figure 3).

In the JEL sediment profile, two lithologies are differentiated. The basal 4 cm and the top 11 cm consist of grey, homogeneous sediments. Between 11 and 46 cm, calcite varves similar to the JG varves are preserved. These are composed of a calcite sublayer including frustules of planktonic diatoms (*Stephanodiscus* spp.) and an organic sublayer consisting of planktonic and epiphytic diatoms and organic debris. Varve thickness ranges from 0.5 to 7 mm/a (Figure 3).

The main difference in varve micro-facies between the three lakes is the occurrence of two varve types (calcite and organic diatom varves) in JG, whereas in JC and JEL only calcite varves are formed. Calcite varves in the JC sediments exhibit a complex structure with up to five seasonal sublayers, whereas calcite varves in JG and JEL represent comparably simple couplets. In particular, distinct sublayers of chrysophyte cysts and thick monospecific diatom layers, pyrite crystals and endogenic calcite patches only formed in JC but not in the JG and JEL sediments. There is also no link between varve thickness maxima of the three records. Another obvious difference is the undisturbed varve preservation at JG,

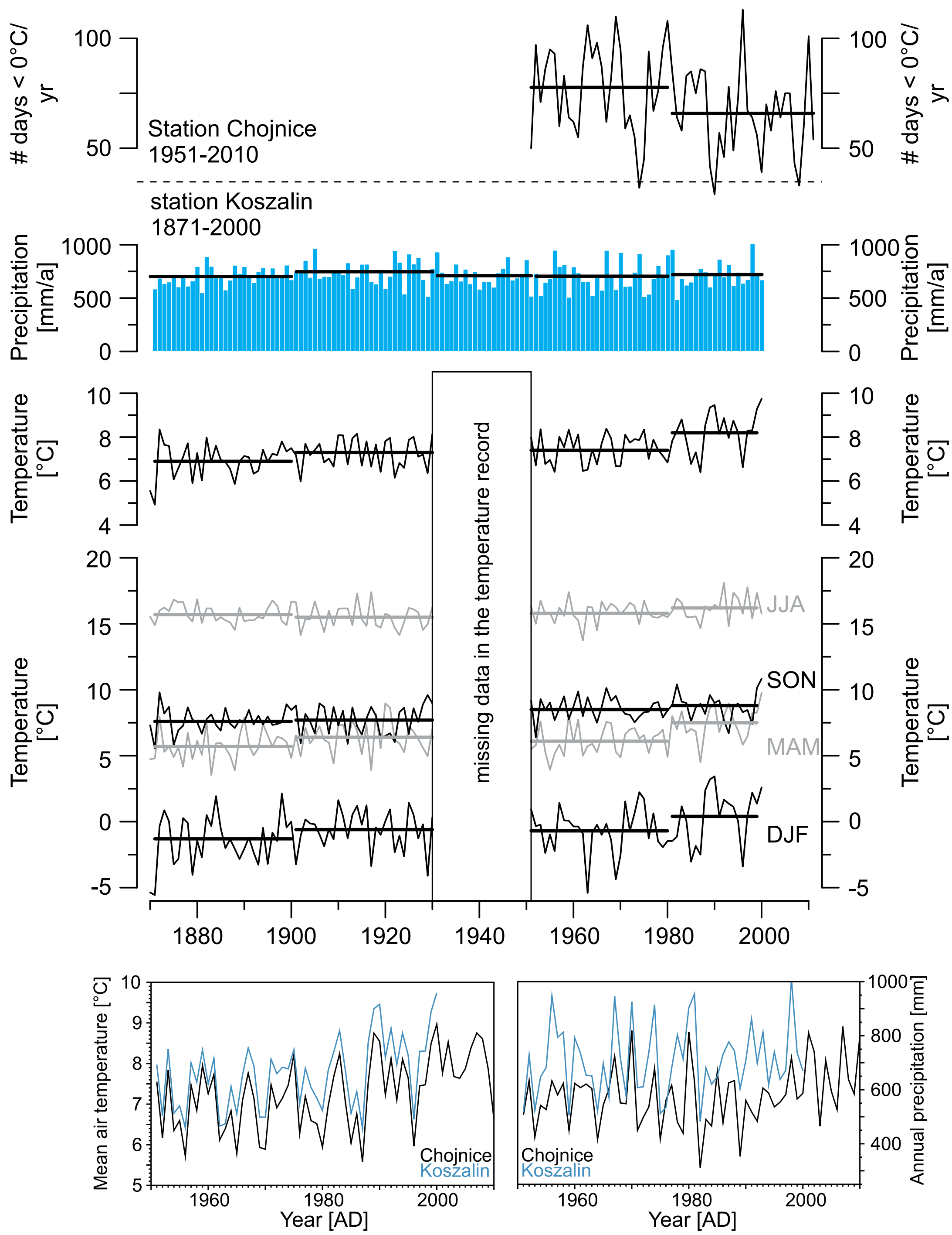

Figure 2. Number of frost days (<0°C) calculated based on the daily mean air temperature data from the climate station Chojnice (53°42′N/17°33′E, 188 m a.s.l.), operated by the Institute of Meteorology and Water Management (IMGW) for the period 1951–2011. Monthly precipitation and mean air temperature data from Koszalin (54°12′N/16°09′E, 34 m a.s.l.) for the period 1871–2000 provided by the Global Historical Climatology Network (GHCN; Peterson and Vose, 1997; Peterson et al., 1998). Temperature data are displayed as annual and seasonal (DJF, MAM, JJA and SON) means. Bold lines indicate the 30-year mean values since 1871.

whereas in the JC record short intervals of faint varve preservation and JEL even non-varved intervals are intercalated.

Chronology

Varve chronology. Microscopic annual layer counting was independently carried for each sediment record in the study intervals. Continuous varve counting for JG revealed a total of 139 (first counting) and 137 (second counting) varves, resulting in a varve chronology from AD 2013 back to AD 1876 ± 2 with a counting uncertainty of 1.4% (Figure 3). For the JC core, a continuous varve chronology comprising a total of 135 (first counting) and 132 (second counting) varves with a counting uncertainty of 2.2% has been established. For two poorly varved sections (26–18 and 11–9 cm), varve numbers have been interpolated. The resulting varve chronology from AD 2010 back to 1877 ± 3 is confirmed by independent ^{137}Cs dating (Figure 3). ^{137}Cs activity concentration measurements have been applied for core JC10-2 and showed two distinct maxima at 16–14 and 10–8 cm sediment depth. Varve counted and interpolated ages for both ^{137}Cs activity concentration maxima revealed the intervals 1958–1963 (16–14 cm) and 1979–1989 (10–8 cm), thus reflecting the atmospheric nuclear weapon testing in the early 1960s and the fallout after the Chernobyl accident in AD 1986, respectively (Figure 3; Putyrskaya

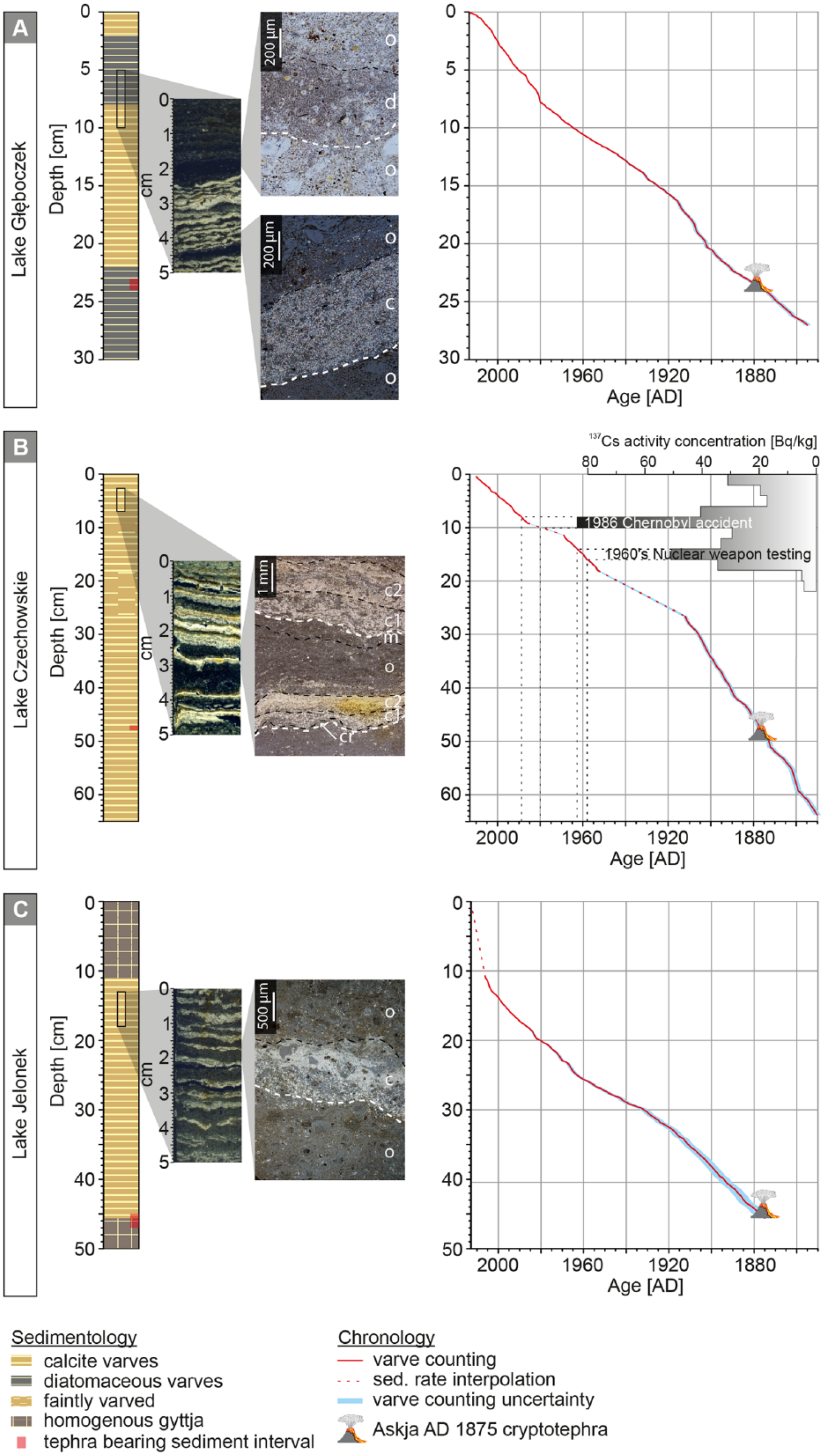

Figure 3. Lithology and age models for Lake Głęboczek (top), Lake Czechowskie (middle) and Lake Jelonek (bottom). Thin section scans and microphotographs display typical varve micro-facies for each lake (c/c1/c2 = calcite sublayer, cr = chrysophyte cysts sublayer, d = diatom sublayer, m = mixed sublayer and o = organic sublayer). Each sediment record was independently dated by a combination of varve counting (red line) and tephrochronology (Askja AD 1875 tephra). JC has been additionally dated by ^{137}Cs activity concentration measurements. Varve counting uncertainty estimates are derived by multiple counting by two different investigators.

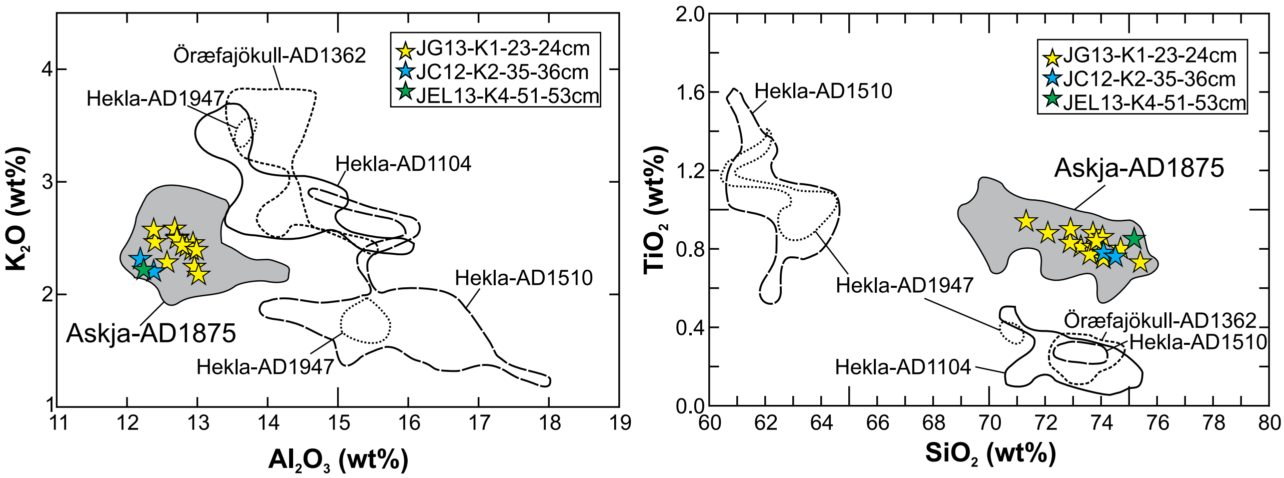

Figure 4. Geochemical biplots of normalized (volatile-free) single glass data of the Askja AD 1875 tephra in Lake Głęboczek (yellow star), Lake Czechowskie (blue star) and Lake Jelonek (green star). EPMA glass reference data are obtained from the following: Andersson et al. (2010), Bergman et al. (2004), Boygle (1998), Dugmore et al. (1995), Eirksson et al. (2000), Larsen et al. (1999, 2002), Óladóttir et al. (2011), Oldfield et al. (1997), Pilcher et al. (1996, 2005), Sigurdsson and Sparks (1978), Stivrins et al. (2016), Tylmann et al. (2016) and Wulf et al. (2016).

et al., 2009). This chronology is further supported by a recent calibration study comparing in situ ^{10}Be concentration at annual resolution from core JC10-7 and neutron monitor data suggesting an uncertainty of ±1 varve year (Czymzik et al., 2015). Varve counting for JEL for the interval from 46 to 11 cm revealed 134 (first counting) and 128 (second counting) varves (4.5% mean counting error). Because of the uppermost homogeneous sediments, the varve chronology is floating (Figure 3) and has been anchored at the Askja AD 1875 tephra with an uncertainty of ±4 varve years because the glass shards have been obtained from a sample containing eight varves. Adding the counting uncertainty, the resulting varve chronology spans from AD 2006 back to 1875 ± 7. The time interval between the upper end of the varved interval at 11 cm sediment depth and the top of the sediment profile (coring year 2013) has been extrapolated. The rather high sedimentation rate of 15 mm/a resulting for the topmost non-varved 11 cm is not unusual for the JEL sediment record. For example, high mean sedimentation rates of about 5 mm/a have been found for the first millennium AD (Filbrandt-Czaja, 2009).

Tephrochronology. Cryptotephra horizons were identified in JG13-K1 (23–24 cm core depth, 25 glass shards), JC12-K2 (35–36 cm core depth, 10 glass shards) and JEL13-K4 (51–53 cm core depth, 5 glass shards). EPMA analyses of 13 (JG), 2 (JC) and 1 (JEL) glass shards revealed a very similar homogeneous composition with ranges in SiO_2 of 71.3–75.4 wt%, TiO_2 of 0.7–0.9 wt%, Al_2O_3 of 12.2–13.0 wt%, FeO of 2.9–4.7 wt%, CaO of 1.8–3.0 wt% and K_2O of 2.2–2.6 wt% (normalized water-free data; Figure 4). The geochemical composition of glass shards in all profiles as well as their stratigraphic position proves a correlation with the Askja AD 1875 eruption from W-Iceland.

Geochemistry

Bulk TOC and calculated $CaCO_3$ (mainly calcite) values for JG vary between 6% and 20% and from 13% to 78%, respectively. Highest TOC values of up to 20% are recorded between 30 and 20 cm and from 8 to 2 cm, while between 20 and 8 cm sediment depth, TOC contents are lower (down to 6%). Highest calcite contents up to 78% are recorded between 22 and 8 cm and from 2 to 0 cm, whereas calcite values decrease down to 13% between 30 and 22 cm and from 8 to 2 cm sediment depth. The Si/Ti and the Ti records are less variable than the TOC and calcite contents (Figure 5).

TOC and $CaCO_3$ contents in the JC sediments fluctuate from 7% to 10% and from 28% to 56%, respectively. TOC values show maxima up to 10% in four intervals at 53–52, 27–17, 12–8 and 4–0 cm. Calcite exhibits lower amplitude fluctuations with highest values up to 56% in the uppermost 9 cm. The Si/Ti and Ti records show low variability despite a maximum in Si/Ti which coincides with a minimum in Ti values from 8 to 5 cm (Figure 4).

TOC and $CaCO_3$ values for JEL range from 14% to 29% and from 8% to 67%, respectively. Highest TOC contents up to 29% and lowest calcite contents of about 8% are recorded for the uppermost 15 cm. Si/Ti ratios and Ti remain stable with slightly increasing (Ti) and decreasing (Si/Ti ratios) trends from 15 cm sediment depth to the sediment surface (Figure 4).

From all three sediment profiles, JG shows highest mean $CaCO_3$ values (54%), followed by JEL (42%) and JC (37%). Mean TOC values are highest in JEL (19%), followed by JG (11%) and JC (8%). According to micro-facies analyses, the remaining sediment components in all three lake records are mainly diatom frustules and subordinated chrysophyte cysts. Detrital components in all three records are very low, as proven by microscopic inspection and the low Ti values. Based on these observations, we broadly estimate the contribution of diatom silica by the following equation: $100 - \%TOC - \%CaCO_3$. We are aware that %TOC does not exactly equal organic matter; however, this uncertainty in our calculation may affect the absolute numbers but not the downcore variability. In result, we found highest diatom silica of ca. 55% for the JC sediments compared with ca. 39% in JEL and 35% in JG. This is confirmed by microscopic observation of thick diatom layers in the JC record and also explains the lower relative calcite and TOC concentrations in JC. The higher contribution of diatom frustules in the JC sediments also contributes to the observed higher sedimentation rate in this record.

Discussion

Proxy signal interpretation

In this paper, we concentrate on sediment micro-facies and geochemical proxies. All investigated records are either entirely (JG and JC) or predominantly (JEL) varved. Varve preservation is interpreted as the absence of post-depositional processes such as bioturbation and erosion (Brauer, 2004; Larsen and MacDonald, 1993; Tylmann et al., 2012; Zolitschka et al., 2015).

The generally low contribution of detrital minerogenic matter from the catchment is evidenced for all records through microscopic analyses and low Ti values. Because of the low amount of siliciclastics, we interpret Si/Ti ratios as proxy for

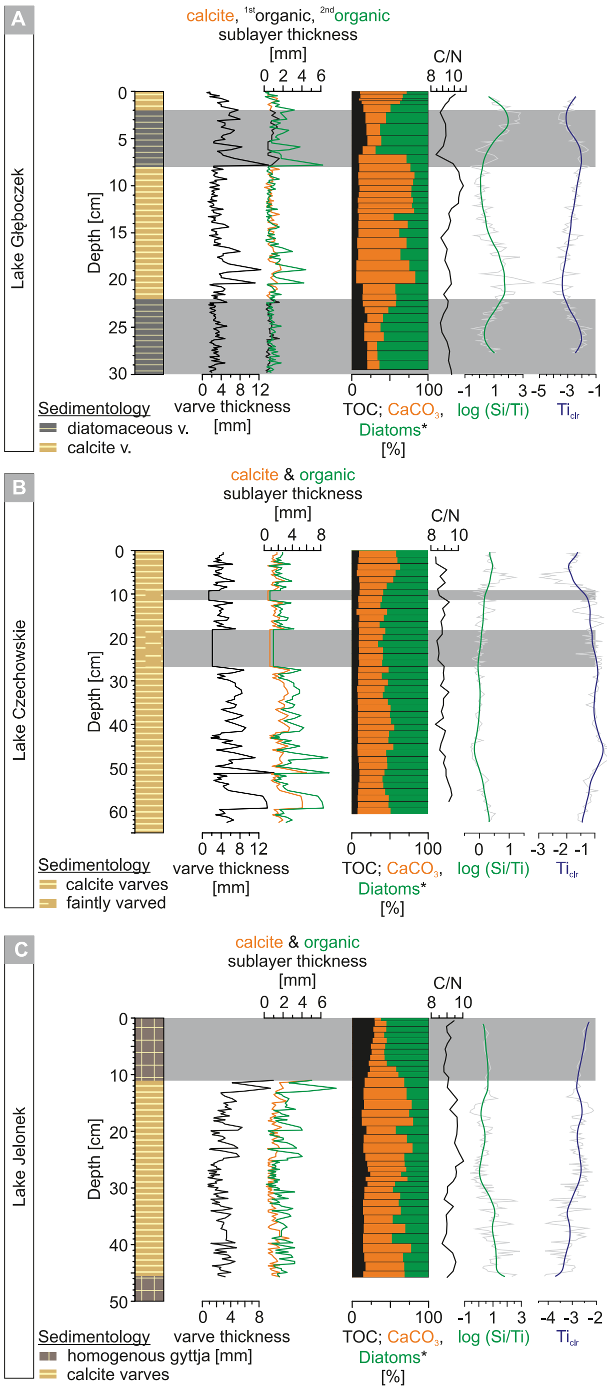

Figure 5. Micro-facies (varve and sublayer thicknesses), bulk geochemical (TOC, $CaCO_3$, diatom contents and C/N ratio) and μ-XRF element data (log(Si/Ti) and Ti_{clr} date displayed as annual and 30-year running mean) for Lake Głęboczek (top), Lake Czechowskie (middle) and Lake Jelonek (bottom). Grey bars indicate sedimentological changes.

diatom abundance, that is, lake productivity (Figure 5). Likely explanations include the absence of major inflowing rivers and the low relief limiting catchment erosion. An additional factor for JC is the core location in eastern sub-basin of the lake, which is separated by a shallow sill from the western sub-basin. Therefore, the western sub-basin acts as a trap for potential inflow of detrital matter from the northern and western part of the catchment (Figure 1). Microscopic analyses show that the main sediment components in all three records are biochemically precipitated calcite, diatoms and organic matter that mainly reflect aquatic biomass as indicated by C/N ratios <10 (Figure 5; Meyers and Teranes, 2001). Except two short intervals of organic-diatomaceous varves in JG, only calcite varves formed in all study lakes. Calcite varves consist of sublayers of biochemically precipitated calcite together with diatom frustules which form during lake water warming in spring (Bluszcz et al., 2008; Kienel et al., 2013, 2017). The occurrence of two subsequent calcite sublayers within one varve indicates two annual pulses of calcite formation probably related to higher primary lake productivity. Sublayers consisting of planktonic diatoms following the calcite deposition reflect a productivity phase during autumn seasons. Exceptionally thick (up to 11 mm), monospecific diatom (*Fragiliaria* spp.) layers, occasionally including endogenic calcite patches, are related to years with strongly enhanced productivity. Mixed sublayers composed of periphytic diatoms (e.g. *Navicula* spp.) and littoral carbonates indicate sediment re-suspension from the littoral likely caused by intensified lake circulation and wave activity. The absence of calcite sublayers (only observed in JG) can either be related to dissolution during settling of the crystals through the water column or to a reduced supply of Ca^{2+} ions (Bluszcz et al., 2008; Dean, 1999). TOC content variations in all three lakes are interpreted as proxy for productivity (Lüder et al., 2006) rather than organic matter preservation (Dräger et al., 2017; Hartnett et al., 1998). This is corroborated by the coincidence of high TOC and diatom contents in all three sediment records. Faint or non-varved intervals only occur in JC and JEL, respectively. For JC, faint varve preservation is likely related to periods of enhanced wind-induced lake circulation. In contrast to the deposition of thick monospecific diatom layers and littoral sediments, which are also related to wind-induced water column mixing, varve preservation ceases where either the duration or the strength of mixing periods increases. For JEL, it might be realistic that not only lake circulation but also changes in the size/depth relation influence oxic/anoxic conditions favouring bioturbation and the absence of varved sediments.

Climatic versus local proxy responses

We compared the changes in sediment proxies in the three lakes records with regional meteorological data. Air temperature increased during the last 140 years in two steps at around 1900 and during the 1970s and 1980s (Figures 2 and 6). Until 1900, the coldest mean annual (6.9°C) and seasonal (DJF: −1.3°C; MAM: 5.7°C; JJA: 15.7°; SON: 6.9°C) air temperatures are recorded and reflect the final phase of the 'LIA' (Grove, 2001; Figures 2 and 6). Until 1900, especially DJF air temperatures show strong interannual variability ranging from −5.9°C to 2.1°C (Figure 2). From 1900 to around 1980, mean annual air temperatures remained rather stable at around 7.4°C. Seasonal air temperatures were also higher compared with the time before 1900 (DJF: −0.7°C; MAM: 6.3°C; JJA: 15.7°C; SON: 8.1°C). Since ca. 1980, mean (8.2°C) and seasonal (DJF: 0.4°C; MAM: 7.5°C; JJA: 16.2°C; SON: 8.8°C) air temperatures increased to highest values in the last 140 years. The accelerated warming since 1980 resulted in a decrease in the length of winter ice cover length (Figure 6), which is seen as a general trend in the entire Baltic Sea realm (Rutgersson et al., 2014).

Annual precipitation increased at around 1900 from 691 to 720 mm/year and remained rather stable since then. A trend to wetter conditions at the onset of the 20th century is also recorded in a peat record from Northern Poland (De Vleeschouwer et al., 2009).

The increasing temperatures in combination with a slight increase in mean annual precipitation at the end of the 'LIA' triggered sedimentological responses in all studied lake records at around AD 1900. The most distinct response is observed in the smallest lake (JG) where at AD 1895 ± 2, sedimentation abruptly changed from organic diatom to calcite varves within 1 year. Possible climatic causes for this change are either increasing temperatures and/or precipitation because biochemical calcite precipitation

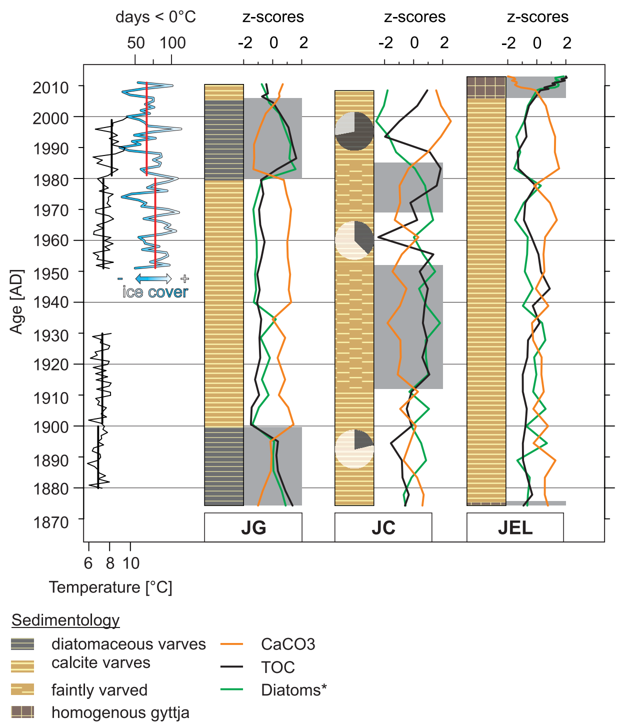

Figure 6. Proxy data compilation for the last 140 years. Temperature data display annual mean temperature from the Koszalin station. The number of frost days is based on temperature data from Chojnice. TOC, $CaCO_3$ and residuals are displayed as normalized z-scores.

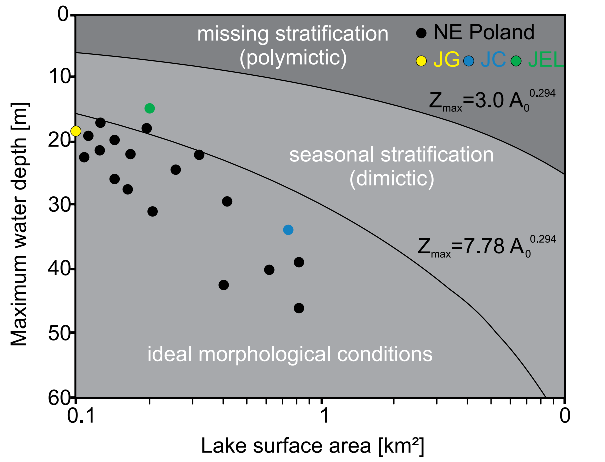

Figure 7. Biplot showing the relation between maximum water depth and lake surface area to lake stratification and the occurrence of varved lake sediments (using the equations by Larsen and MacDonald, 1993; modified after Tylmann et al., 2013). The dots indicate varved lake sediments in north-eastern Poland (black; Tylmann et al., 2013), north-central Poland with Lake Głęboczek (JG, dark blue), Lake Czechowskie (JC, blue) and Lake Jelonek (JEL, green) (all this study).

is favoured by warmer temperatures and by the supply of Ca^{2+} ions through runoff and groundwater flow (Kelts and Hsü, 1978; Koschel et al., 1983). Since continuous calcite varve formation in the neighbouring lake site JC indicates that regional temperatures were sufficient for calcite precipitation even during the late 'LIA', we suggest that an increase in precipitation might have triggered the onset of calcite precipitation at JG. In contrast to JC, where Ca^{2+} was always sufficient for calcite precipitation due to the larger catchment, we speculate that Ca^{2+} ion concentrations in JG are limited because of the smaller catchment (Figures 1 and 7). Therefore, even small-scale climatic changes leading to an enhanced supply in Ca^{2+} might have been sufficient to trigger the onset of calcite varve formation at JG. Similar processes have been previously reported from other lakes with limitations in Ca^{2+} ions (Martin-Puertas et al., 2017; Schettler et al., 1999). If our hypothesis could be confirmed, this would be a good example for a depositional system close to an internal threshold that is a sensitive recorder even of minor climatic changes. However, an ultimate proof of a lake-internal threshold for climate change remains difficult (Williams et al., 2011).

The sediment response in JC to the AD 1900 warming is less distinct because of the aforementioned reason and calcite varves continuously formed over the entire study interval. Because of the large catchment, JC is sufficiently supplied by Ca^{2+} ions, allowing continuous calcite precipitation (Bluszcz et al., 2008; Dean, 1999). The increase in TOC contents at around 1900 might be interpreted as a temperature-driven increase in productivity, but we cannot exclude human-induced eutrophication either. Interestingly, varve preservation decreased ca. 10 years later and is accompanied by an increase in re-suspended sediments. This might be either related to lake-level fluctuations or to more intense water circulation. The latter might be favoured by the large surface area that makes the lake prone to wind-driven water circulation, but because wind data for this period are lacking, this interpretation remains elusive.

JEL does not exhibit visible changes in sedimentological proxies at AD 1900. However, a major change from non-varved to varved sediments occurred already at AD 1875. This might reflect an earlier, threshold type of response to climate warming at the end of the LIA compared with the other two lakes, likely related to the higher surface area/depth ratio of JEL at the limit of favourable conditions for varve preservation (Figure 7). For this reason, JEL is more sensitive to varve formation and preservation than JC and JG.

The phase of accelerated warming starting between the 1970s and 1980s is strongly seen in JG with the shift from calcite to organic varves from one to the next year. Interestingly, this is the opposite sediment response to warming than observed at about AD 1900, when organic varves were replaced by calcite varves. This non-linear proxy response to warming might be related to calcite dissolution favoured by further increased warming. Higher temperatures since 1980 and especially mild winters with short ice cover duration, shown by a decreasing number of frost days (Figure 6), likely caused an increased organic biomass production (Hargeby et al., 2004; Kosten et al., 2009). The resulting enhanced decomposition of organic matter and increase in CO_2, in turn, decreased pH values and, thereby, favoured calcite dissolution (Dean, 1999) as observed in SEM images. Slower settling of organic particles due to the temperature-driven strength and duration of the water column stratification might have further reinforced this effect. As a result, calcite dissolution processes could already start within the metalimnion (Bluszcz et al., 2008).

In the JC sediment record, only a subtle change in varve microfacies is observed. Since about 1991 in an increasing number of years, varves with two calcite formation phases were deposited (Figure 6), indicating higher primary productivity likely caused by extended periods of lake productivity due to warmer spring and autumn seasons. In particular, spring temperatures increased since 1980 (7.5°C) compared with the period prior 1980 (6.3°C). Extended periods of lake productivity are also seen in the occurrence of thick monospecific diatom layers occurring occasionally throughout the last 140 years. The increasing degree of varve preservation at around 1985 might be either related to more stable lake stratification or to the increased forest cover in the catchment (Figure 8) which decreased wind-driven lake circulation.

JEL sediments do not show a clear proxy response to the recent warming. Only TOC contents and diatoms slightly increase since about 1980, which might suggest increasing lake productivity due to increasing temperatures.

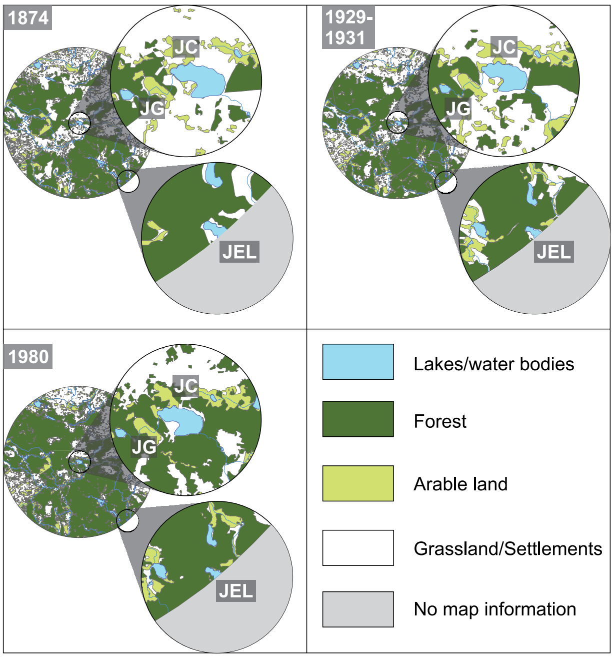

Figure 8. Compilation of vegetation cover changes for three time periods (1874, 1929–1931 and 1980). Maps were created using historic maps and aerial/satellite imagery.

The most distinct change in sediment deposition to two phases of increasing temperature during the last 140 years is observed at the smallest lake JG. JC sediments only show an attenuated response. The onset of varve formation at JEL might have benefited from climate warming, but no further sediment responses due to climate change have been observed. The sensitivity of JG sedimentation to climate change likely is related to its morphological conditions of lake and catchment size and water depth (Figure 7). It enables continuous varve preservation, and the small catchment size (65 ha), together with the isolated location with respect to human settlements, amplifies sediment responses to regional climate changes. However, the differences in varve responses to increasing warming around 1900 and 1980 point to a non-linear proxy-forcing relation that needs to be investigated further.

The attenuated sedimentation response to recent warming in JC likely is due to the large lake size and its location at the end of a lake cascade including JG resulting in a comparably large catchment area. Moreover, JC is the only of the three study lakes with human settlements on the lake shore, which might have additionally influenced lake sedimentation. However, as for JG and JEL, we do not observe changes (increases) in detrital material flux and, therefore, exclude a major impact of anthropogenic activity on the runoff regime and erosion. Afforestation in the JC catchment since the 1980s probably had an indirect effect on sediment formation because of the increase in wind shelter through increasing tree cover of near-shore areas.

The surface area/water depth ratio of JEL is responsible for the discontinuous varve preservation (Figure 7). JEL's location is also isolated with no human settlements in the close vicinity. The surface area/catchment size ratio (0.18) is similar to JG (0.11), whereas JEL is lacking a clear sediment response to the observed climate changes. The shallower water depth enhances the potential of superimposing the regional climate signals.

Conclusion

Three neighbouring varved lake records have been investigated for their sedimentation responses to climatic warming in the last 140 years. The sediment records have been precisely synchronized using the Askja AD 1875 tephra, an isochrone at the end of the 'LIA'. Detrital sediment flux due to erosion is negligible in the three lakes and indicates only minor human impact, making these lakes particularly suitable for investigating regional climate versus local lake control of proxy data.

The clear response of varve micro-facies to climate warming in only one of the study lakes (JG), in comparison with the attenuated (JC) or less clear (JEL) response in the others, points to the importance of site-specific factors for sedimentation. It further suggests that the observed recent changes mainly in JG and to a lesser degree in JC do not exceed changes in sedimentation observed as consequences of warming at the end of LIA. Most likely, the driver for varve micro-facies changes at JG is a combination of the small size of the lake and the catchment and the lack of major human impact, enhancing the lake's sensitivity mainly to changes in precipitation because this controls groundwater flow and ion concentration in the lake water. In contrast, JC is more sensitive towards wind stress driving water circulation and sediment re-suspension mainly because of its larger size and large shallow water areas. The occurrence of non-varved intervals only in JEL likely is due to the larger ratio of lake size to water depth. Therefore, an unambiguous response to climate forcing is not recorded.

This study demonstrates the value of high-resolution lake comparison based on precise tephra-based synchronization for better constraining proxy data responses to climate and environment changes. Our results show that these, at first glance, similar lakes show rather different sensitivities towards climate forcing because of specific lake-internal thresholds. However, their quantification remains difficult and needs to be tested on longer timescales and for additional lakes.

Acknowledgements

The authors thank the coring team (Brian Brademann and Robert Schedel) for excellent core recovery; Dieter Berger, Gabi Arnold and Brian Brademann for thin section preparation; and Manuela Dziggel and Andreas Hendrich for help with the figure design.

Funding

This study is a contribution to the Virtual Institute of Integrated Climate and Landscape Evolution Analyses (ICLEA), grant number VH-VI-415, and the climate initiative REKLIM Topic 8 'Schnelle Klimaänderungen aus Proxydaten' of the Helmholtz Association and the National Science Centre (Poland), grant number 2011/01/B/ST10/07367.

References

Andersson S, Rosqvist G, Leng MJ et al. (2010) Late-Holocene climate change in central Sweden inferred from lacustrine stable isotope data. *Journal of Quaternary Science* 25(8): 1305–1316.

Bergman J, Wastegård S, Hammarlund D et al. (2004) Holocene tephra horizons at Klocka Bog, west-central Sweden: Aspects of reproducibility in subarctic peat deposits. *Journal of Quaternary Science* 19(3): 241–249.

Bluszcz P, Kirilova E, Lotter AF et al. (2008) Global radiation and onset of stratification as forcing factors of seasonal carbonate and organic matter flux dynamics in a hypertrophic Hardwater Lake (Sacrower See, Northeastern Germany). *Aquatic Geochemistry* 14(1): 73–98.

Bonk A, Kinder M, Enters D et al. (2016) Sedimentological and geochemical responses of Lake Żabińskie (north-eastern Poland) to erosion changes during the last millennium. *Journal of Paleolimnology* 56(2–3): 239–252.

Boygle J (1998) A little goes a long way: Discovery of a new mid-Holocene tephra in Sweden. *Boreas* 27: 195–199.

Brauer A (2004) Annually laminated lake sediments and their paleoclimatic relevance. In: Fischer H, Kumke T, Lohmann G and et al. (eds) *The Climate in Historical Times: Towards a Synthesis of Holocene Proxy Data and Climate Models* (GKSS School of Environmental Research). Berlin: Springer-Verlag, pp. 111–129.

Brauer A and Casanova J (2001) Chronology and depositional processes of the laminated sediment record from Lac d' Annecy, French Alps*. *Journal of Paleolimnology* 25: 163–177.

Brauer A, Endres C and Negendank KFW (1999a) Late glacial calendar year chronology based on annually laminated sediments from Lake Meerfelder Maar, Germany. *Quaternary International* 61: 17–25.

Brauer A, Endres C, Gu C et al. (1999b) High resolution sediment and vegetation responses to Younger Dryas climate change in varved lake sediments from Meerfelder Maar, Germany. *Quaternary Science Reviews* 18: 321–329.

Brauer A, Hajdas I, Blockley SPE et al. (2014) The importance of independent chronology in integrating records of past change for the 60-8 ka INTIMATE time interval. *Quaternary Science Reviews* 106: 47–66.

Brauer A, Mangili C, Moscariello A et al. (2008) Palaeoclimatic implications from micro-facies data of a 5900 varve time series from the Piànico interglacial sediment record, southern Alps. *Palaeogeography, Palaeoclimatology, Palaeoecology* 259(2–3): 121–135.

Błaszkiewicz M (2005) *Późnoglacjalna i wczesnoholoceńska ewolucja obniżeń jeziornych na Pojezierzu Kociewskim (wschodnia część Pomorza)*. Warszawa: IGiPZ PAN.

Błaszkiewicz M, Piotrowski JA, Brauer A et al. (2015) Climatic and morphological controls on diachronous postglacial lake and river valley evolution in the area of Last Glaciation, northern Poland. *Quaternary Science Reviews* 109: 13–27.

Croudace IW, Rindby A and Rothwell RGUY (2006) ITRAX: Description and evaluation of a new multi-function X-ray core scanner. In: Rothwell RG (ed.) *New Techniques in Sediment Core Analysis*. London: Geological Society of London (Special Publications), pp. 51–63.

Czymzik M, Brauer A, Dulski P et al. (2013) Orbital and solar forcing of shifts in Mid- to Late-Holocene flood intensity from varved sediments of pre-alpine Lake Ammersee (southern Germany). *Quaternary Science Reviews* 61: 96–110.

Czymzik M, Muscheler R, Brauer A et al. (2015) Solar cycles and depositional processes in annual 10Be from two varved lake sediment records. *Earth and Planetary Science Letters* 428: 44–51.

Davies SM (2015) Cryptotephras: The revolution in correlation and precision dating. *Journal of Quaternary Science* 30: 114–130.

De Vleeschouwer F, Piotrowska N, Pawlyta J et al. (2009) Multiproxy evidence of 'Little Ice Age' palaeoenvironmental changes in a peat bog from northern Poland. *The Holocene* 19(4): 625–637.

Dean WE (1999) The carbon cycle and biogeochemical dynamics in Lake sediments. *Journal of Paleolimnology* 21: 375–393.

Degirmendžić J, Kozuchowski K and Zmudzka E (2004) Changes of air temperature and precipitation in Poland in the period 1951–2000 and their relationship to atmospheric circulation. *International Journal of Climatology* 24: 291–310.

Dräger N, Theuerkauf M, Szeroczyńska K et al. (2017) Varve microfacies and varve preservation record of climate change and human impact for the last 6000 years at Lake Tiefer See (NE Germany). *The Holocene* 27(3): 450–464.

Dugmore AJ, Larsen GR and Newton AJ (1995) Seven tephra isochrones in Scotland. *The Holocene* 5(3): 257–266.

Eirksson J, Knudsen KL, Haflidason H et al. (2000) Chronology of late-Holocene climatic events in the northern North Atlantic based on AMS 14C dates and tephra markers from the volcano Hekla, Iceland. *Journal of Quaternary Science* 15(6): 573–580.

Filbrandt-Czaja A (2009) *Studia nad historia szaty róslinnej i krajobrazu Borow Tuchólskich*. Torun: Wydawnictwo Naukowe Uniwersytetu Mikołaja Kopernika.

Filipiak J and Mietus M (2009) Spatial and temporal variability of cloudiness in Poland, 1971–2000. *International Journal of Climatology* 29: 1294–1311.

Goslar T (1995) High concentration of atmospheric 14C during the Younger Dryas cold episode. *Nature* 377(5): 414–417.

Grove JM (2001) The initiation of the 'Little Ice age' in regions round the North Atlantic. *Climatic Change* 48: 53–82.

Hargeby A, Blindow I and Hansson M (2004) Shifts between clear and turbid states in a shallow lake: Multi-causal stress from climate, nutrients and biotic interactions. *Archiv für Hydrobiologie* 161(4): 433–454.

Hartnett HE, Keil RG, Hedges JI et al. (1998) Influence of oxygen exposure time on organic carbon preservation in continental margin sediments. *Nature* 391: 572–575.

Kämpf L, Brauer A, Swierczynski T et al. (2014) Processes of flood-triggered detrital layer deposition in the varved Lake Mondsee sediment record revealed by a dual calibration approach. *Journal of Quaternary Science* 29(5): 475–486.

Kelts K and Hsü KJ (1978) Freshwater carbonate sedimentation. In: Lerman A (ed.) *Lakes – Chemistry, Geology, Physics*. Berlin: Springer-Verlag, pp. 295–323.

Kienel U, Dulski P, Ott F et al. (2013) Recently induced anoxia leading to the preservation of seasonal laminae in two NE-German lakes. *Journal of Paleolimnology* 50(4): 535–544.

Kienel U, Kirillin G, Brademann B et al. (2017) Effects of spring warming and mixing duration on diatom deposition in deep Tiefer See, NE Germany. *Journal of Paleolimnology* 57(1): 37–49.

Killick R and Eckley IA (2014) changepoint: An R Package for changepoint analysis. *Journal of Statistical Software* 58(3): 1–15.

Kordowski J, Błaszkiewicz M, Kramkowski M et al. (2014) Charakterystyka środowisk depozycyjnych Jeziora Czechowskiego i jego otoczenia [Characteristics of depositional environments of Czechowskie Lake basin and its vicinity]. *Landform Analysis* 25: 55–75.

Koschel R, Benndorf J, Proft G et al. (1983) Calcite precipitation as a natural control mechanism of eutrophication. *Archiv für Hydrobiologie* 98: 380–408.

Kosten S, Kamarainen A, Jeppesen E et al. (2009) Climate-related differences in the dominance of submerged macrophytes in shallow lakes. *Global Change Biology* 15(10): 2503–2517.

Lane CS, Brauer A, Blockley SPE et al. (2013) Volcanic ash reveals time-transgressive abrupt climate change during the Younger Dryas. *Geology* 1251–1254.

Larsen CPS and MacDonald GM (1993) Lake morphometry, sediment mixing and the selection of sites for fine resolution palaeoecological studies. *Quaternary Science Reviews* 12: 781–792.

Larsen G, Dugmore A and Newton A (1999) Geochemistry of historical-age silicic tephras in Iceland. *The Holocene* 9(4): 463–471.

Larsen G, Eiríksson J, Knudsen KL et al. (2002) Correlation of late-Holocene terrestrial and marine tephra markers, north Iceland: Implications for reservoir age changes. *Polar Research* 21(2): 283–290.

Latalowa M, Pedziszewska A, Maciejewska E et al. (2013) Tilia forest dynamics, Kretzschmaria deusta attack, and mire hydrology as palaeoecological proxies for mid-Holocene climate reconstruction in the Kashubian Lake District (N Poland). *The Holocene* 23(5): 667–677.

Lauterbach S, Brauer A, Andersen N et al. (2011) Multi-proxy evidence for early to mid-Holocene environmental and climatic changes in NE Poland. *Boreas* 40: 57–72.

Lowe DJ (2011) Tephrochronology and its application: A review. *Quaternary Geochronology* 6(2): 107–153.

Lüder B, Kirchner G, Lücke A et al. (2006) Palaeoenvironmental reconstructions based on geochemical parameters from annually laminated sediments of Sacrower See (northeastern Germany) since the 17th century. *Journal of Paleolimnology* 35: 897–912.

Luterbacher J, Xoplaki E, Küttel M et al. (2010) Climate change in Poland in the past centuries and its relationship to European climate: Evidence from reconstructions and coupled climate models. In: Przybylak R, Majorowicz J, Brázdil R et al. (eds) *The Polish Climate in the European Context: An Historical Overview*. New York: Springer, pp. 3–39.

Marks L (2012) Timing of the Late Vistulian (Weichselian) glacial phases in Poland. *Quaternary Science Reviews* 44: 81–88.

Martin-Puertas C, Brauer A, Dulski P et al. (2012) Testing climate–proxy stationarity throughout the Holocene: An example from the varved sediments of Lake Meerfelder Maar (Germany). *Quaternary Science Reviews* 58: 56–65.

Martin-Puertas C, Tjallingii R, Bloemsma M et al. (2017) Varved sediment responses to early Holocene climate and environmental changes in Lake Meerfelder Maar (Germany) obtained from multivariate analyses of micro X-ray fluorescence core scanning data. *Journal of Quaternary Science* 32(3): 427–436.

Meyers PA and Teranes JL (2001) Sediment organic matter. In: Last WM and Smol JP (eds) *Tracking Environmental Change Using Lake Sediments – Volume 2: Physical and Geochemical Methods*. Dordrecht: Kluwer Academic Publisher, pp. 239–269.

Neugebauer I, Brauer A, Schwab MJ et al. (2015) Evidences for centennial dry periods at 3300 and 2800 cal. yr BP from micro-facies analyses of the Dead Sea sediments. *The Holocene* 25(8): 1358–1371.

Ojala AEK, Francus P, Zolitschka B et al. (2012) Characteristics of sedimentary varve chronologies – A review. *Quaternary Science Reviews* 43: 45–60.

Óladóttir BA, Larsen G and Sigmarsson O (2011) Holocene volcanic activity at Grimsvötn, Bárdarbunga and Kverkfjöll subglacial centres beneath Vatnajökull, Iceland. *Bulletin of Volcanology* 73(9): 1187–1208.

Oldfield F, Thompson R, Crooks PRJ et al. (1997) Radiocarbon dating of a recent high latitude peat profile: Stor Amyran, northern Sweden. *The Holocene* 7(3): 283–290.

Olsen J, Anderson NJ and Leng MJ (2012) Limnological controls on stable isotope records of late-Holocene palaeoenvironment change in SW Greenland: A paired lake study. *Quaternary Science Reviews* 66: 85–95.

Ott F, Wulf S, Serb J et al. (2016) Constraining the time span between the Early Holocene Hässeldalen and Askja-S Tephras through varve counting in the Lake Czechowskie sediment record, Poland. *Journal of Quaternary Science* 31(2): 103–113.

Pędziszewska A, Tylmann W, Witak M et al. (2015) Holocene environmental changes reflected by pollen, diatoms, and geochemistry of annually laminated sediments of Lake Suminko in the Kashubian Lake District (N Poland). *Review of Palaeobotany and Palynology* 216: 55–75.

Peterson TC and Vose RS (1997) An overview of the global historical climatology network temperature database. *Bulletin of the American Meteorological Society* 78: 2837–2849.

Peterson TC, Vose R, Schmoyer R et al. (1998) Global historical climatology network (GHCN) quality control of monthly temperature data. *International Journal of Climatology* 1179: 1169–1179.

Pilcher J, Bradley R, Francus P et al. (2005) A Holocene tephra record from the Lofoten Islands, Arctic Norway. *Boreas* 34(2): 136–156.

Pilcher JR, Hall VA and McCormac FG (1996) An outline tephrochronology for the Holocene of the north of Ireland. *Journal of Quaternary Science* 11(6): 485–494.

Putyrskaya V, Klemt E and Röllin S (2009) Migration of 137Cs in tributaries, lake water and sediment of Lago Maggiore (Italy, Switzerland) – Analysis and comparison with Lago di Lugano and other lakes. *Journal of Environmental Radioactivity* 100(1): 35–48.

Roberts N, Allcock SL, Arnaud F et al. (2016) A tale of two lakes: A multi-proxy comparison of Lateglacial and Holocene environmental change in Cappadocia, Turkey. *Journal of Quaternary Science* 31(4): 348–362.

Rutgersson A, Jaagus J, Schenk F et al. (2014) Observed changes and variability of atmospheric parameters in the Baltic Sea region during the last 200 years. *Climate Research* 61(2): 177–190.

Schettler G, Rein B and Negendank JFW (1999) Geochemical evidence for Holocene palaeodischarge variations in lacustrine records from the Westeifel Volcanic Field, Germany: Schalkenmehrener Maar and Meerfelder Maar. *The Holocene* 9(4): 381–400.

Sigurdsson H and Sparks RSJ (1978) Rifting episode in north Iceland in 1874–1875 and the eruptions of Askja and Sveinagja. *Bulletin Volcanologique* 41(3): 149–167.

Słowiński M, Błaszkiewicz M, Brauer A et al. (2015) The role of melting dead ice on landscape transformation in the early Holocene in Tuchola Pinewoods, North Poland. *Quaternary International* 388: 64–75.

Słowiński M, Zawiska I, Ott F et al. (2017) Differential proxy responses to late Allerød and early Younger Dryas climatic change recorded in varved sediments of the Trzechowskie palaeolake in Northern Poland. *Quaternary Science Reviews* 158: 94–106.

Stivrins N, Wulf S, Wastegård S et al. (2016) Detection of the Askja AD 1875 cryptotephra in Latvia, Eastern Europe. *Journal of Quaternary Science* 31(5): 437–441.

Tjallingii R, Röhl U, Kölling M et al. (2007) Influence of the water content on X-ray fluorescence core-scanning measurements in soft marine sediments. *Geochemistry, Geophysics, Geosystems* 8(2): 1–12.

Tylmann W, Bonk A, Goslar T et al. (2016) Calibrating 210Pb dating results with varve chronology and independent chronostratigraphic markers: Problems and implications. *Quaternary Geochronology* 32: 1–10.

Tylmann W, Szpakowska K, Ohlendorf C et al. (2012) Conditions for deposition of annually laminated sediments in small meromictic lakes: A case study of Lake Suminko (northern Poland). *Journal of Paleolimnology* 47(1): 55–70.

Tylmann W, Zolitschka B, Enters D et al. (2013) Laminated lake sediments in northeast Poland: Distribution, preconditions for formation and potential for paleoenvironmental investigation. *Journal of Paleolimnology* 50(4): 487–503.

Wacnik A, Tylmann W, Bonk A et al. (2016) Determining the responses of vegetation to natural processes and human impacts in north-eastern Poland during the last millennium: Combined pollen, geochemical and historical data. *Vegetation History and Archaeobotany* 25(5): 479–498.

Weltje GJ and Tjallingii R (2008) Calibration of XRF core scanners for quantitative geochemical logging of sediment cores: Theory and application. *Earth and Planetary Science Letters* 274(3–4): 423–438.

Weltje GJ, Bloemsma MR, Tjallingii R et al. (2015) Prediction of Geochemical Composition from XRF Core Scanner Data: A New Multivariate Approach Including Automatic Selection of Calibration Samples and Quantification of Uncertainties. In: Croudace IW and Rothwell RG (eds) *Micro-XRF Studies of Sediment Cores: Applications of a Non-Destructive Tool for the Environmental Sciences*. Berlin: Springer, pp. 507–534.

Wibig J (1999) Precipitation in Europe in relation to circulation patterns at the 500 hPa level. *International Journal of Climatology* 19: 253–269.

Williams JW, Blois JL and Shuman BN (2011) Extrinsic and intrinsic forcing of abrupt ecological change: Case studies from the late Quaternary. *Journal of Ecology* 99(3): 664–677.

Wulf S, Dräger N, Ott F et al. (2016) Holocene tephrostratigraphy of varved sediment records from Lakes Tiefer See (NE Germany) and Czechowskie (N Poland). *Quaternary Science Reviews* 132: 1–14.

Wulf S, Ott F, Słowiński M et al. (2013) Tracing the Laacher See Tephra in the varved sediment record of the Trzechowskie palaeolake in central Northern Poland. *Quaternary Science Reviews* 76: 129–139.

Yu G and Harrison SP (1995) Holocene changes in atmospheric circulation patterns as shown by lake status changes in northern Europe. *Boreas* 24: 260–268.

Zolitschka B, Francus P, Ojala AEK et al. (2015) Varves in lake sediments – A review. *Quaternary Science Reviews* 117: 1–41.